

OBSERVATIONS ON INTERNALLY
OXIDIZED SILVER-MAGNESIUM
AND SILVER-ALUMINUM ALLOYS

J.S. Hirschhorn and F.V. Lenel

TO BE SUBMITTED TO ASM
TRANSACTIONS QUARTERLY

[REDACTED]

OBSERVATIONS ON INTERNALLY OXIDIZED
SILVER-MAGNESIUM AND SILVER-ALUMINUM ALLOYS

by

J. S. Hirschhorn and F. V. Lenel

J. S. Hirschhorn former graduate student at Rensselaer Polytechnic Institute is presently Assistant Professor of Metallurgical Engineering in the Minerals and Metals Engineering Department, University of Wisconsin, Madison, Wisconsin. F. V. Lenel is Professor and Chairman of the Materials Engineering Department, Rensselaer Polytechnic Institute. This paper is based on a Ph.D. thesis submitted by J. S. Hirschhorn to the Department of Materials Engineering, Rensselaer Polytechnic Institute, Troy, New York.

Abstract

Silver-magnesium alloys containing 1 and 2 at. % Mg and a silver-2 at. % aluminum alloy were internally oxidized under conditions causing rapid rates of oxidation and uniform structures to be formed. The microhardness and lattice parameter of the oxidized alloys were measured and they increased linearly with decreasing oxidation temperature in the range of 600 to 900°C. The annealing behavior of the alloy with 2 at. % Mg was studied. The hardness and lattice parameter decreased to constant values during annealing at temperatures above the oxidation temperature. The final values of hardness and lattice parameter were the same as the values for materials oxidized directly at the annealing temperature. Annealing at a temperature below the oxidation temperature did not affect the hardness or lattice parameter. Transmission electron microscopic examination of the Ag-2 at. % Mg alloy yielded evidence for the presence of a fine dispersion of oxide particles. It is proposed that the changes in hardness and lattice parameter are related to changes in the morphology of the oxide dispersion.




Figure Captions

- Figure 1. Hardness or lattice parameter versus velocity.
- Figure 2. Hardness versus oxidation temperature for Ag-Mg alloys.
- Figure 3. Lattice parameter versus oxidation temperature for Ag-Mg alloys.
- Figure 4. Effect of oxidation temperature on hardness of Ag-2.0 at. % Al alloy.
- Figure 5. Lattice parameter versus oxidation temperature for Ag-Al alloy.
- Figure 6. Annealing curves for Ag-2.0 at. % Mg alloy oxidized at 700°C.
- Figure 7. Annealing curves for Ag-2.0 at. % Mg alloy oxidized or pre-annealed at 800°C.
- Figure 8. Hardness versus oxidation and annealing temperature for Ag-2.0 at. % Mg alloy.
- Figure 9. Lattice parameter versus oxidation and annealing temperature for Ag-2.0 at. % Mg alloy.
- Figure 10. Electron micrograph of Ag-2.0 at. % Mg alloy internally oxidized at 900°C. (111,000X)
- Figure 11. Electron diffraction pattern of Ag-2.0 at. % Mg alloy internally oxidized at 900°C; points A, B and C correspond to (220), (311) and (222) type reflections from oxide phase and point D denotes ring passing through (200) diffraction spots from matrix. (2.4X)

Figure 12. Electron diffraction pattern of annealed unoxidized Ag-2.0 at. % Mg alloy. (2.2X)

Figure 13. Electron diffraction pattern of Ag-2.0 at. % Mg alloy internally oxidized at 600°C and annealed at 900°C for 6-1/4 hours; points A, B and C correspond to (400), (331) and (420) type reflections from oxide phase and point D denotes (111) ring from matrix. (3X)

Observations on Internally Oxidized Silver-Magnesium and Silver-Aluminum Alloys

The increases in the hardness and lattice parameter of internally oxidized dilute (less than 3 at. %) Ag-Mg and Ag-Al alloys have been determined in several investigations (1-7). Bosch et al (5) determined the hardness and lattice parameter as a function of the rate of oxidation (i.e., velocity of the oxidation boundary) at 900°C for Ag-Mg alloys. It was observed that both the hardness and lattice parameter increased with increasing boundary velocity until a critical velocity value was reached; at higher than critical velocities the hardness and lattice parameter remained constant. Additional work was also carried out at some lower oxidation temperatures (6,8). The results are summarized schematically in Figure 1.

The present study examined the dependence of the maximum hardness and lattice parameter, which could be obtained at any given oxidation temperature, on the oxidation temperature for Ag-1 at. % Mg, Ag-2 at. % Mg and Ag-2 at. % Al alloys. In order to ascertain the thermal stability of the oxidized materials, specimens of the Ag-2 at. % Mg alloy were annealed at temperatures below and above the oxidation temperature. The results are compared to previous observations on such materials.

One of the major obstacles to a complete understanding of the structure-property relationships for such internally oxidized materials has been the difficulty of observing the second phase oxide particles

which are produced during internal oxidation. Several recent studies (7, 9, 10) involving transmission electron microscopy have yielded direct evidence for the existence of such particles in internally oxidized Ag-Mg and Ag-Al alloys. A limited amount of evidence was also obtained in the present study and these results are compared to the results of the previous investigations.

Experiments

Alloy Preparation The alloys used in this study were prepared in the same manner as those used by Bosch et. al. (5) and the details of the melting and casting process have been given elsewhere (8, 11). The nominal compositions of the alloys were 1 and 2 at. % Mg and 2 at. % Al; the exact chemical analysis, as determined by Handy and Harmon and given in Table I, show that the low Mg content alloy actually contained 1.3 at. % Mg while the other two agreed with the nominal values.

The cast ingots which were 5/8 inches in diameter and 6 inches long were cold swaged to 1/4 inch diameter rod and the rods rolled into strips 0.010 or 0.020 inches thick and 3/8 inches wide. After suitable degreasing the strip specimens were annealed for at least one hour in argon at about one atmosphere of pressure at 900°C. Zirconium foil was also present in order to remove any oxygen present. This treatment resulted in complete recrystallization and a grain size of about 0.25 mm.

Internal Oxidation and Annealing

The results of Bosch et al (5) showed that above a critical velocity of the oxidation front the measured properties became independent of the velocity. It was assumed that these results were correct and that if such alloys were internally oxidized in a high enough oxygen pressure, then the total range of velocities in the specimen would be above the critical value. The actual velocity (v) of the oxidation boundary is related to the variables of the process by the following equation which has been derived by several authors (2, 12, 13):

$$v = \frac{C_o D_o}{C_m \times R} \quad \text{Eq. 1}$$

where C_o is the concentration of oxygen at the surface, D_o is the oxygen diffusivity, C_m is the alloy solute concentration, X is the distance beneath the sheet surface, and R the ratio of oxygen to metal atoms in the oxide formula. The experimental data (14) relating C_o to the partial pressure of oxygen (p_o) has the form

$$C_o = k p_o^{1/2} \quad \text{Eq. 2}$$

where k is a numerical constant dependent on temperature. Calculations based on Eqs. 1 and 2 and the data on the solubility of oxygen in Ag of Steacie and Johnson (14) were made to determine the necessary pressure of oxygen to obtain a minimum velocity, corresponding to the center of the sheet, which was appreciably greater than the appropriate critical velocity above which the hardness and lattice parameter become independent of velocity.

Specimens were oxidized at a pressure of 6.4 atmospheres of pure oxygen. Metallographic examination of the specimens showed them to be completely oxidized, as evidenced by a thin boundary line down the center of the specimen cross section. In addition, microhardness values were independent of depth below the surface; hence, the correctness of the procedure was indicated.

Internal oxidation was carried out by inserting a specimen into a quartz boat inside a quartz tube which was closed at one end and at the other end bolted against a brass manifold by means of an O-ring. The brass manifold had connections through solenoid valves with a vacuum pump and an oxygen cylinder. The quartz tube was then evacuated and a three zone furnace (consisting of three separate nichrome windings on a ceramic tube) at the desired temperature was then placed around the tube. The current to each winding was controlled separately. The temperature of the furnace over a length of at least four inches was controlled to within $\pm 2^{\circ}\text{C}$ over the temperature range of 500 to 900°C . Oxygen at the desired pressure was then admitted into the quartz tube. The time of oxidation was normally from 15 to 30 minutes. The oxygen was then evacuated and the furnace removed from the quartz tube.

Annealing of oxidized specimens was carried out in the same furnace arrangement, except that the quartz tube was open to the atmosphere.

Metallography Following internal oxidation, specimens were mounted and prepared by normal metallographic techniques. The etchant used was an aqueous solution of 2% each of chromic and sulfuric acids. The internal oxidation boundaries were clearly delineated.

Certain specimens were examined by transmission electron microscopy which also allowed electron diffraction patterns to be obtained. In order to prepare foils suitable for transmission of electrons and free from surface films, which are usually formed on such materials, the following procedure was used. An electropolishing technique was developed in which the bath consisted of an aqueous solution containing 4% KCN, 4% K_2CO_3 , and 4% AgCN. The solution was in a beaker which was immersed in an ice bath. The cathodes consisted of pointed Ag wires perpendicular to the two faces of the specimen. The cathode to specimen distance was about 1/2 inch. The voltage was normally between 15 and 20 volts. The specimen was agitated by tapping the copper wire to which it was attached.

It was necessary to use a particular optimum voltage which was that value at which the current remained approximately constant. This observation was an important one because the power source was not continuously on. Following a suggestion of Swann et al (9), the current was supplied from the D.C. source in pulses of about 0.2 seconds duration at a frequency of about 2 pulses per second. During optimum electrothinning the current oscillated between zero and a particular value which depended on the specimen size. In addition to pulsing the current, the electrothinning was carried out in cycles. The pulsing current was kept on for 20 to 60 seconds and kept off for similar periods. The purpose of the pulsing and cycling was to keep film formation on the specimen to a minimum.

More material was removed from one side of the specimen so that the material observed in the electron microscope did not represent the exact center of the original specimen, which might have become depleted of solute during oxidation. Areas near the smallest visible holes produced in the foils were prepared for examination in a Hitachi-HU-11 electron microscope operated at 100 KV. The major difficulty in such examinations was the lack of large thin areas and the reduction in clarity and resolution due to the "oxydy" surfaces of the materials. Selected area diffraction patterns were also obtained.

Hardness Hardness values were obtained with a Kentron microhardness tester, a Knoop indenter and an applied load of 100 gms. The average of from 15 to 40 readings on any given specimen was obtained.

X-Ray Diffraction Measurements A Phillips diffractometer and nickel filtered copper radiation were used to determine the lattice parameters of the materials. Instrument alignment was assured by measuring the lattice parameter of pure Ag; this was found to be 4.0858 \AA which is in good agreement with accepted values. Actual lattice parameters were determined by calculating parameters corresponding to individual diffraction peaks and plotting them versus $\cos^2 \theta$, where θ is the Bragg angle, and extrapolating a straight line through the data points to $\cos^2 \theta = 0$. The accuracy of the determined lattice parameters was about $\pm 0.0003 \text{ \AA}$. The widths of diffraction peaks at 1/2 of the maximum intensity were measured in order to determine the presence of line broadening.

Experimental Results

Hardness and Lattice Parameter Both the microhardness and lattice parameter of the Ag-1.3 at. % Mg, Ag-2 at. % Mg, and the Ag-2 at. % Al alloys oxidized in the form of 10 mil thick strips were determined for various oxidation temperatures in the range of 600 to 900°C. These results are shown in Figures 2-5. It is seen that both microhardness and lattice parameter increase linearly with decreasing oxidation temperature.

A series of annealing treatments were carried out on the Ag-2 at. % Mg alloy. The microhardness was carefully measured on such materials in order to determine the effect of both annealing time and temperature on the original oxidized material. The first set of experiments were performed on specimens which were oxidized at 700°C. The annealing temperatures were 775, 800, 850 and 900°C, and the results are shown in Figure 6. Annealing resulted in decreases in the microhardness until a critical time was reached, after which the hardness was unaffected by further annealing.

A second series of experiments were performed on specimens which were oxidized at 800°C and the annealing temperatures were 850 and 900°C; the results are shown in Figure 7. In addition to these materials, a specimen from the previous set of experiments which was annealed at 800°C was given a second annealing treatment at 900°C, and these data are also shown in Figure 7.

The final mean hardness values of the annealed materials are shown as a function of the annealing temperature in Figure 8 together with the data on hardness as a function of oxidation temperature for this Ag-2 at. % Mg alloy. It is seen that all the data fit on one line. No annealing experiments were carried out on the Ag-1.3 at. % Mg or Ag-2 at. % Al alloys because of the smaller dependence of hardness on oxidation temperature.

The lattice parameters of the specimens of the first set of annealing experiments were determined after the hardness of these materials had reached their final values. These values are shown in Figure 9 as a function of the annealing temperature together with lattice parameter values as a function of the oxidation temperature for this same alloy. It is seen that all the data fit on the same straight line.

In order to detect any effect of annealing at a temperature below the original oxidation temperature a specimen oxidized at 900°C was annealed at 800°C for 14-1/4 hours. There was no change in the hardness or lattice parameter of the material.

The previous work of Bosch et al (5) and Oswald (6) indicated that at low oxidation temperatures (e.g. 500°C) the maximum attainable hardness for the Ag-2 at. % Mg alloy could be obtained from oxidation in air. Accordingly, a 20 mil thick specimen of this alloy was oxidized in air at 500°C for 62 hours. The measured hardness was 254 KHN, the highest observed hardness for this alloy, and the hardness was constant throughout the cross section of the specimen. The hardness of this

specimen is plotted in Figure 8 and it is seen that the data point falls on the same line as the other data. The surface of this specimen was somewhat unusual. The grain structure was made visible because of the fact that each grain was slightly bulged outward from the surface. Microscopic examination indicated that there was some degree of intercrystalline fracture in the material in the as-oxidized condition. The specimen was extremely fragile and no x-ray diffraction work was possible. However, these observations would indicate that the lattice parameter increase in this material was that which would be indicated by extrapolating the data of Figure 9 to 500 °C.

A specimen similarly oxidized at 500°C in air was also given an annealing treatment at 800°C for 24 hours. The annealed hardness was found to be 194 KHN and constant throughout the cross section; this value is also plotted in Figure 9. This data point also falls on the straight line drawn ^{through} the other data.

Line Broadening The widths of several orders of diffraction lines at 1/2 maximum intensity were measured for various materials. The results are given in Table II. It is seen that no line broadening was observed for oxidized specimens as compared to pure annealed Ag or an annealed unoxidized alloy.

Electron Microscopy The best transmission electron micrograph obtained in the present study is given by Figure 10. There is a uniform distribution of approximately spherical particles in the Ag-2 at. % Mg

alloy oxidized at 900°C. Measurements made on this micrograph and on others with less clarity yielded an average value of 55 Å for the radius of the oxide particles in this alloy. Almost all the particles fall within the size range of 50 to 60 Å radius. A selected area diffraction pattern of this specimen is given in Figure 11. If the particles seen in the transmission micrograph are actually the oxide phase, then there should be some evidence of this phase in the diffraction pattern. Careful examination of the pattern revealed that there were diffraction spots which were not from the Ag matrix. These spots were of extremely low intensity and are difficult to reproduce. Nevertheless, some of these spots are noted in Figure 11.

Because of the poor quality of the films used for electron microscopy, and particularly the poor surfaces usually found, a specimen of the unoxidized Ag-2 at. % Mg alloy was thinned down in exactly the same manner as the oxidized materials. Unexpectedly, the surfaces of the film of the unoxidized material were of a poorer quality than those of the oxidized materials. Electron diffraction patterns obtained for the unoxidized material did not contain any of the extra diffraction spots. Figure 12 is a typical diffraction pattern from this unoxidized material.

On the basis of the results obtained on the unoxidized material it was concluded that the extra diffraction spots observed in the pattern of the oxidized material were due to the same second phase observed in the electron micrographs, and that this second phase

was not due to any type of surface contamination effect. Instead, this second phase must be the oxide phase formed during internal oxidation.

Examination of the material oxidized at 600°C and annealed at 900°C for 6-1/4 hours also revealed some evidence for the presence of a second phase. Although the quality of the transmission micrograph was poor, measurements yielded an average radius value of 60 Å for the second phase particles. A selected area diffraction pattern of this specimen also contained extra diffraction spots not due to the matrix, and this pattern is given in Figure 13.

A micrograph of a Ag-2 at. % Mg specimen oxidized at 600°C was also obtained. In this case there were extremely small low intensity grey spots throughout the micrograph which were believed to be second phase particles. Measurements made on this micrograph indicated that the average radius was about 10 Å. There were also a number of larger particles with radii of about 20 to 30 Å.

There were sufficient extra electron diffraction spots from the oxide phase to allow indexing by routine methods (15). It was found that the ten reflections found on the two patterns, Figures 11 and 13, corresponded to a material with a face-centered-cubic crystal structure. The lattice parameters obtained from the patterns were 9.15 and 8.96 Å for the material oxidized at 900°C and for the material oxidized at 600°C and annealed at 900°C, respectively. The accuracy of the lattice parameter determination is about 0.2 Å. The experimental and theoretical interplanar spacings corresponding to the diffraction

spots from the oxide phase are given in Table III. It is seen that there is very good agreement, indicating that the indexing of the diffraction data was correct.

Discussion

The increases in hardness and lattice parameter, and their dependence on oxidation temperature, observed in this study are in general agreement with previous investigations. Increases in the hardness and lattice parameter of internally oxidized Ag-Mg alloys have been observed in a number of studies (2, 3, 5, 6). However, previous to the present study there were very little data concerning the exact dependence of these increases on oxidation temperature. The observations in this study on the presence of very small discrete oxide particles in the oxidized Ag-Mg alloys indicate that the increases in hardness and lattice parameter of these materials must be related to the presence and morphology of the oxide particles. There was some evidence to indicate that the particle size increased with increasing oxidation temperature. Brimhall and Huggins (10) also obtained transmission micrographs, of about the same quality as those obtained in this study, for internally oxidized Ag-0.5 at. % Mg materials. They too observed very small oxide particles, about 50 Å in radius, and some increase in particle size with increasing oxidation temperature. In general it has been observed, in other alloy systems with much larger oxide particles, that the size of the particles increases with increasing oxidation temperature (16-18). Thus, it appears that both the

hardness and lattice parameter of these materials increase with decreasing oxide particle size. The earlier results concerning the dependence of hardness and lattice parameter on oxidation velocity would indicate that the morphology of the oxide phase is also influenced by the rate of oxidation. In order to produce materials with a uniform structure, one must insure a constant boundary velocity or a range of velocities which are above a critical value.

The increase in hardness and lattice parameter of internally oxidized Ag-Al alloys has also been observed in several studies (1-4, 7). However, the temperature dependence of these increases did not appear to resemble that of the Ag-Mg materials. Darken (7) reported that there was no dependence of the hardness on oxidation temperature for alloys containing 0.4 and 1.9 at. % Al when oxidized in the temperature range of 350 to 850°C. These materials were oxidized under conditions which probably resulted in nonuniform low rates of oxidation within the specimens; hence, the structure of any one specimen was probably nonuniform. The results of the present study clearly indicate that both the hardness and lattice parameter increase with decreasing oxidation temperature. Evidence for the presence of discrete oxide particles in such materials has been given by Darken (7) and Swann (9). Here too the particles were spherical and extremely small. The particles ranged in size from about 15 to 75 Å in radius as determined by direct measurement on transmission micrographs. It is concluded that the structure and properties of the oxidized Ag-Al and Ag-Mg materials are very similar.

The strains present in the oxidized materials as evidenced by the increases in the lattice parameter over the values either for pure silver or for Ag-Mg or Ag-O solid solutions must result from the dispersion of the very small oxide particles. The fact that there is no x-ray line broadening suggests that the strains in the matrix are uniformly distributed throughout macroscopic regions such that the interplanar spacings are increased in a homogeneous fashion and result in a shift of the diffraction lines without any broadening (19). The two phase material may be considered as analogous to substitutional solid solutions (20, 21).

These increases in lattice parameter are most probably due to coherency between the oxide particles and the matrix. The presence of coherency is suggested by the observations of strain contrast in transmission electron micrographs by Brimhall and Huggins (10) and to a limited extent in some of the micrographs obtained in the present study. Additionally, there were only a small number of diffraction spots and not rings attributable to the oxide phase in the electron diffraction patterns, and this indicates that the particles are not randomly oriented.

Although the structure of the oxide phase in the Ag-Mg materials was found to be face-centered-cubic, as is bulk MgO, the lattice parameter was much greater than the 4.2 \AA for bulk MgO. It is believed that this result indicates that the oxide phase may be an Mg-Ag-O complex oxide. Many such ternary oxides exist with this crystal structure and have lattice parameters in the range of 8.0 to 9.3 \AA . The much larger lattice parameter of the oxide phase in comparison to the Ag matrix does not preclude the

existence of coherency between the two materials. The important factor is that there should be interplanar spacings in each phase which are nearly equal. In the present study the observed spacings of the Ag matrix {111} planes, for the Ag-2 at. % Mg material either oxidized at 900°C or oxidized at 600°C and annealed at 900°C, is 2.36 Å and the spacing of the oxide {222} planes is about 2.61 Å. This phenomenon has also been observed in internally oxidized Cu-Al alloys which contain γ -alumina particles, face-centered-cubic with a parameter of 7.9 Å, which are found to be coherent with the Cu matrix (22). The observation that the particles are preferentially oriented in the matrix also supports this interpretation.

It should also be noted that Darken (7) has reported that the oxide phase formed in internally oxidized Ag-Al alloys does not correspond to bulk alumina. Evidence was presented to show that the ratio of oxygen to aluminum atoms in the oxide was greater than the 1.5 associated with Al_2O_3 . This could result from the formation of a complex ternary oxide. The situation is by no means fully understood, but apparently it is likely that the internal oxidation process may result in the formation of oxides which are not observed in bulk form. This seems to be particularly true for the systems in which extremely small oxide particles are formed.

The observations on the annealing behavior of the oxidized Ag-2 at. % Mg alloy indicate that there is a change in the morphology of the oxide dispersion during annealing at temperatures above the oxidation temperature. The fact that constant values of both hardness and lattice parameter are attained, and that these values are exactly the same as for

the material oxidized at the annealing temperature, suggest that there is some kind of particle coarsening process taking place during annealing and oxidation and that some type of equilibrium particle size is reached. Further work is necessary for a complete explanation of this phenomenon. Other studies have also made note of observations which support this interpretation (2, 10, 23, 24).

The results of the present study have pointed out the lack of our complete understanding of the internal oxidation process. It would be advantageous to have a complete theory which could relate the morphology of the oxide dispersion to the oxidation temperature, rate of oxidation, solute content, and annealing time and temperature. Such a theory, although somewhat speculative has been formulated, and will be presented in a separate paper. Another area to be further investigated is the exact relationships between the properties and structures of these oxidized materials. Additional experimental work is being carried out on the room and elevated temperature mechanical properties of these materials.

Acknowledgment

The support of this work by the National Aeronautics and Space Administration is gratefully acknowledged. Mr. C. J. Barton and Mr. G. Leverant were of much assistance during the investigation.

References

1. J. C. Chaston, J. Inst. Metals, 71(1945) 23.
2. J. L. Meijering and M. J. Druyvestyn, Phillips Research Reports, 2 (1947) 81, 260.
3. V. Gottardi, Metallurgia Italiana, 44 (1952) 424.
4. E. Gregory and G. C. Smith, J. Inst. Metals, 85 (1956-57) 81.
5. R. A. Bosch, F. V. Lenel and G. S. Ansell, ASM Trans. Quart., 57 (1964) 960.
6. R. Oswald, Master's Thesis, Rensselaer Polytechnic Institute (1964).
7. L. S. Darken, ASM Trans. Quart., 54 (1961) 599.
8. J. S. Hirschhorn, Ph.D. Thesis, Rensselaer Polytechnic Institute (1965).
9. P. R. Swann, S. Weissmann and D. F. Wriedt, Trans. AIME, 230 (1964) 1306.
10. J. L. Brimhall and R. A. Huggins, Trans. AIME, 233 (1965) 1076.
11. R. A. Bosch, Ph.D. Thesis, Rensselaer Polytechnic Institute (1963).
12. L. S. Darken, Metals Technology, TP 1479 (1942).
13. F. N. Rhines, Trans. AIME, 137 (1940) 318.
14. E. W. R. Steacie and F. M. G. Johnson, Proc. Roy. Soc., 112A (1926) 542.
15. G. Thomas, Transmission Electron Microscopy for Metals, Wiley, New York (1964).
16. W. M. Schwarzkopf, Z. Elektrochemie, 63 (1959) 830.
17. M. S. Ali and V. A. Phillips, Trans. AIME, 215 (1959) 340.

18. O. Preston and N. J. Grant, Trans. AIME, 221 (1961) 164.
19. C. S. Barrett, Structure of Metals, McGraw-Hill, New York (1952).
20. J. Friedel, Adv. in Physics, 3 (1954) 446.
21. A. Guinier, in Solid State Physics, F. Seitz and D. Turnbull, eds., Academic Press, New York, vol. 9 (1959).
22. W. F. Ashby and G. C. Smith, J. Inst. Metals, 9 (1962-63) 182.
23. M. J. Klein and R. A. Huggins, Trans. ASM, 55 (1962) 259.
24. R. Busch, Master's Thesis, U. Calif. (Berkeley, 1963).

Table I

Composition of the Silver-Magnesium
and Silver-Aluminum Alloys

Nominal Composition	Wet Chemical Analysis, wt %			Spectrographic Estimates, ppm				
	<u>Mg</u>	<u>Al</u>	<u>Ag</u>	<u>Cu</u>	<u>Cd</u>	<u>Fe</u>	<u>Pb</u>	<u>Si</u>
Ag + 1 at. % Mg (0.24 wt. %)	0.30		99.70	500	10	20	50	trace
Ag + 2 at. % Mg (0.47 wt. %)	0.48		99.56	300	100	100	trace	trace
Ag + 2 at. % Al (0.50 wt. %)		0.52	99.50	500	10	50	50	trace

Table II

X-Ray Line Broadening Data

Alloy	Treatment	Width at 1/2 Maximum Intensity, arbitrary units		
		(111)	(220)	(311)
Pure Ag	annealed	3.7	4.4	6.7
2 at. % Mg	annealed	4.0	4.8	6.3
1 at. % Mg	oxidized at 600°C	4.0	4.5	6.8
1 at. % Mg	oxidized at 700°C	3.8	4.4	6.8
2 at. % Mg	oxidized at 600°C	3.7	5.0	6.7
2 at. % Mg	oxidized at 800°C	4.1	4.7	6.7
2 at. % Mg	oxidized at 900°C	4.3	5.3	7.0
2 at. % Al	oxidized at 600°C	4.1	5.1	6.2
2 at. % Al	oxidized at 700°C	4.0	4.0	6.4
2 at. % Al	oxidized at 800°C	3.1	5.1	6.0

Table III

Interplanar Spacings (\AA) of Oxide Phase

Specimen	Ag-2.0 at. % Mg oxidized at 900°C		Ag-2.0 at. % Mg oxidized at 600°C; annealed at 900°C	
	<u>d exp.</u>	(a) <u>d theor.</u>	<u>d exp.</u>	(b) <u>d theor.</u>
hkl				
200	4.46	4.58		
220	3.27	3.24		
311	2.86	2.76		
222	2.61	2.64		
400	2.26	2.29	2.22	2.24
331			2.05	2.06
333			1.77	1.72
531			1.53	1.51
442			1.47	1.49
444			1.28	1.29

(a) Theoretical d spacings calculated on the basis of $a_0 = 9.15 \text{ \AA}$.

(b) Theoretical d spacings calculated on the basis of $a_0 = 8.96 \text{ \AA}$.

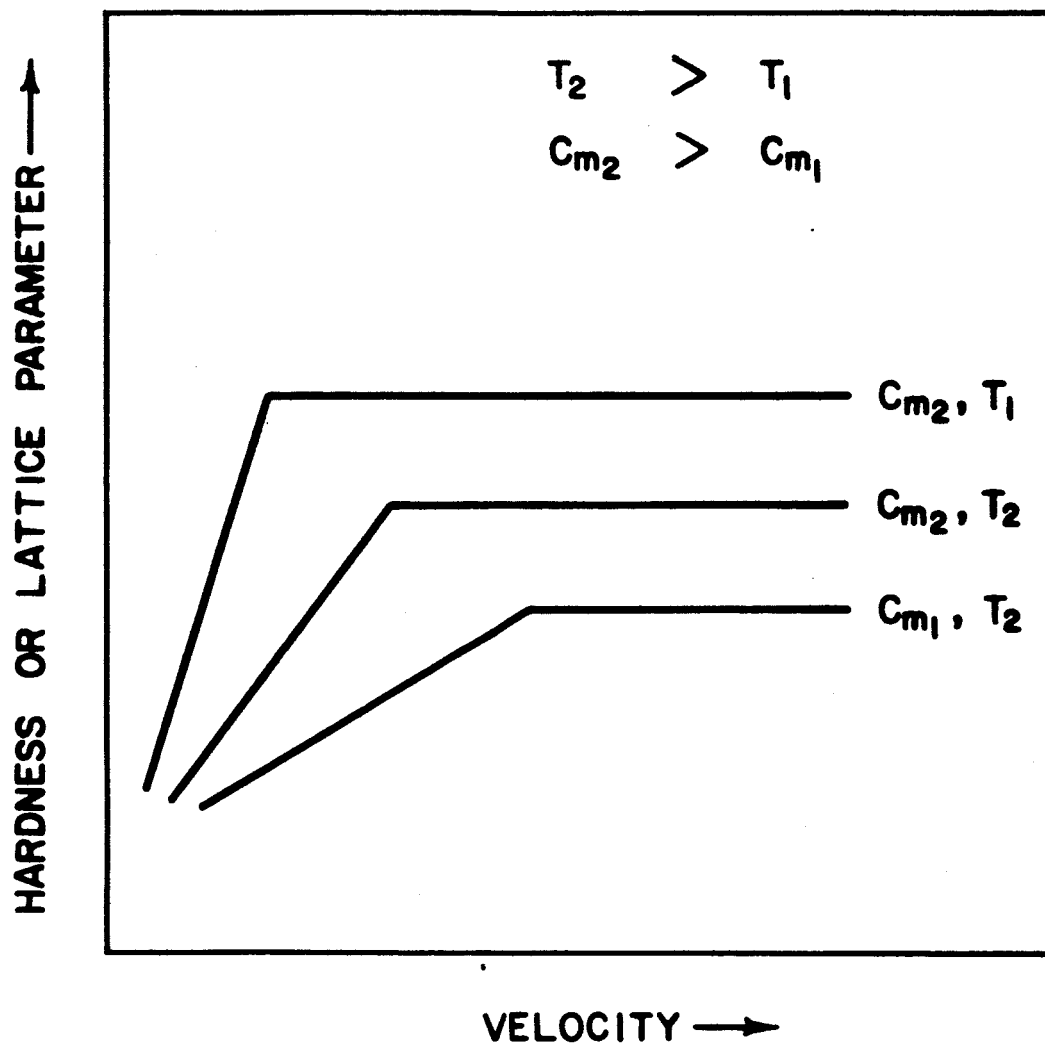


FIGURE 1. HARDNESS OR LATTICE
PARAMETER VERSUS VELOCITY

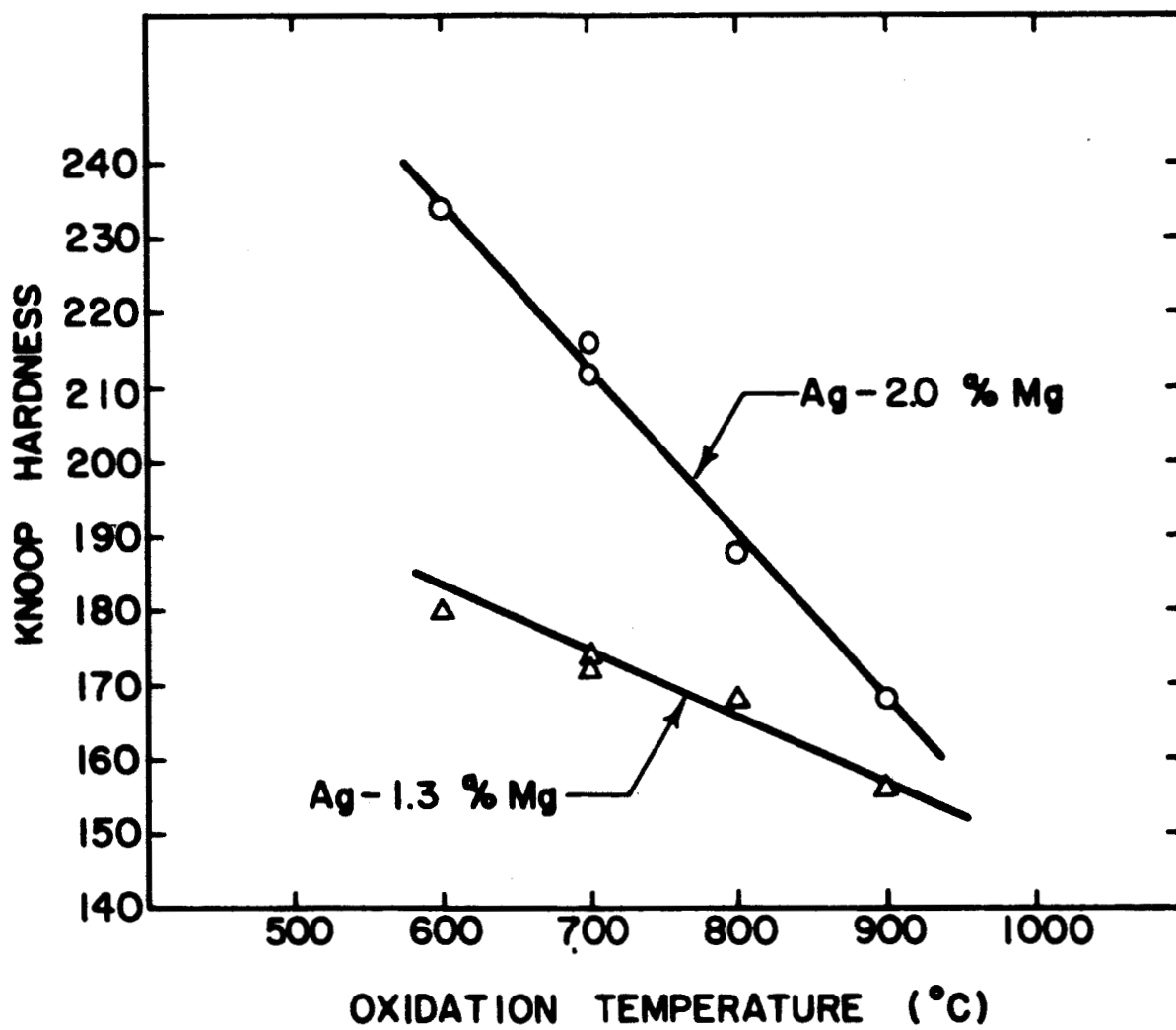


FIGURE 2. HARDNESS VERSUS OXIDATION TEMPERATURE FOR Ag-Mg ALLOYS

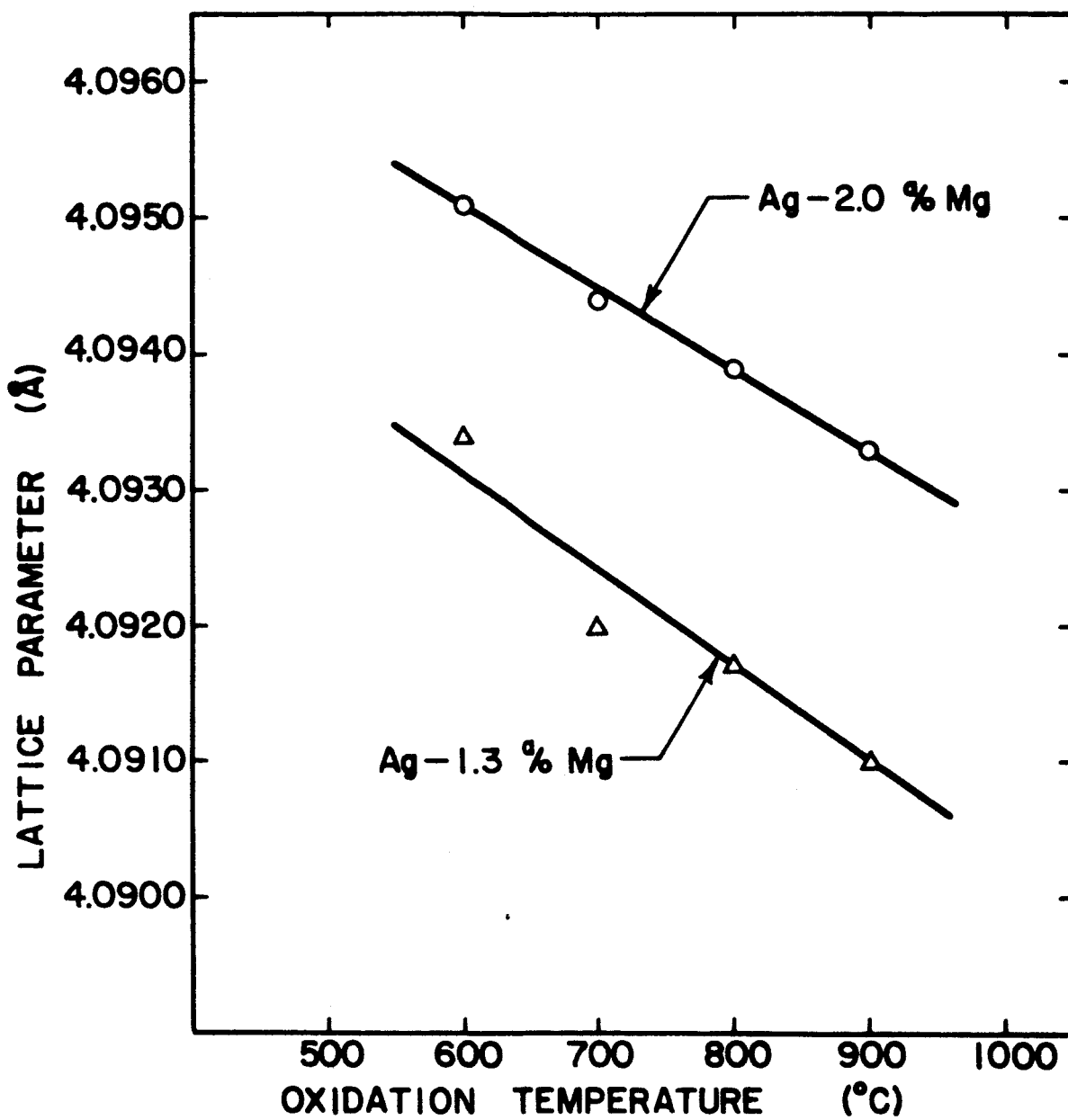


FIGURE 3. LATTICE PARAMETER VERSUS OXIDATION TEMPERATURE FOR Ag-Mg ALLOYS

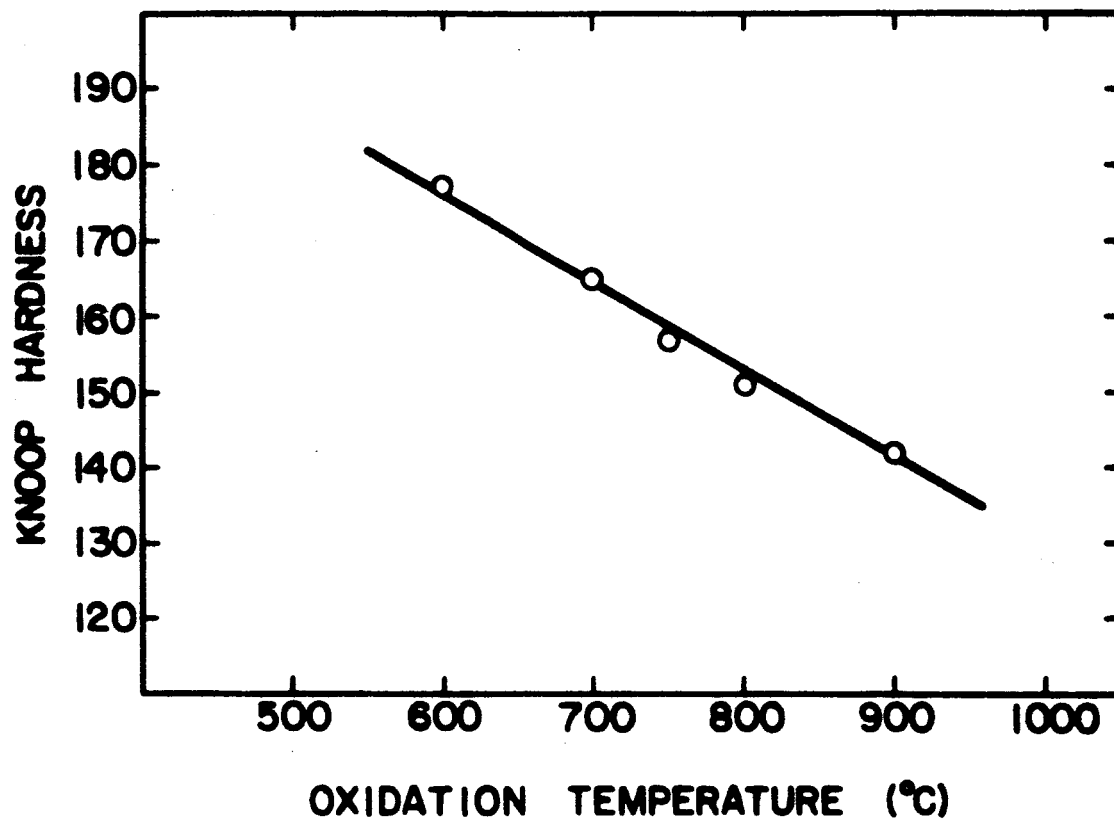


FIGURE 4. EFFECT OF OXIDATION TEMPERATURE ON HARDNESS OF Ag-2.0 % Al ALLOY

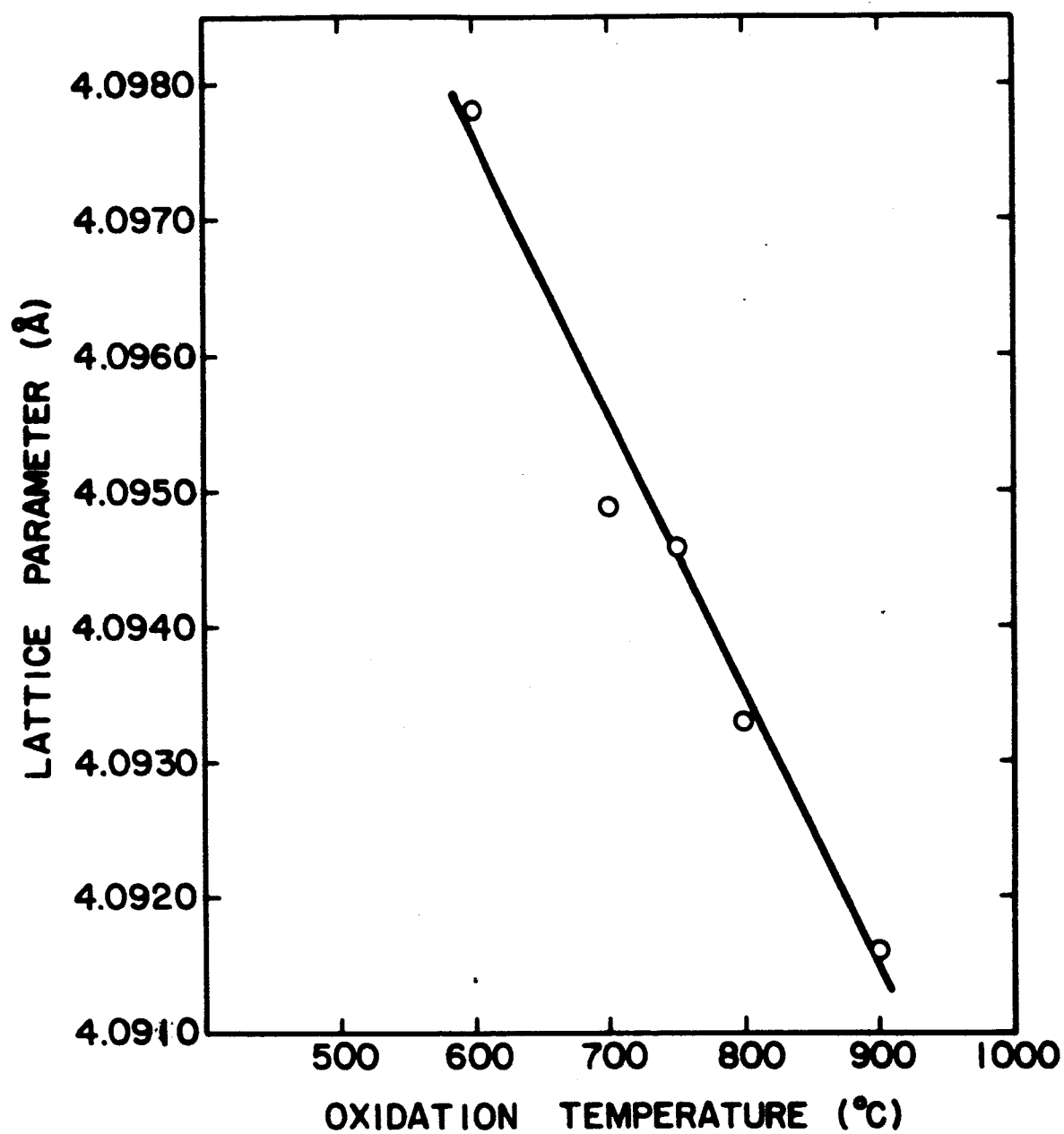


FIGURE 5. LATTICE PARAMETER VERSUS
OXIDATION TEMPERATURE FOR Ag-AI ALLOY

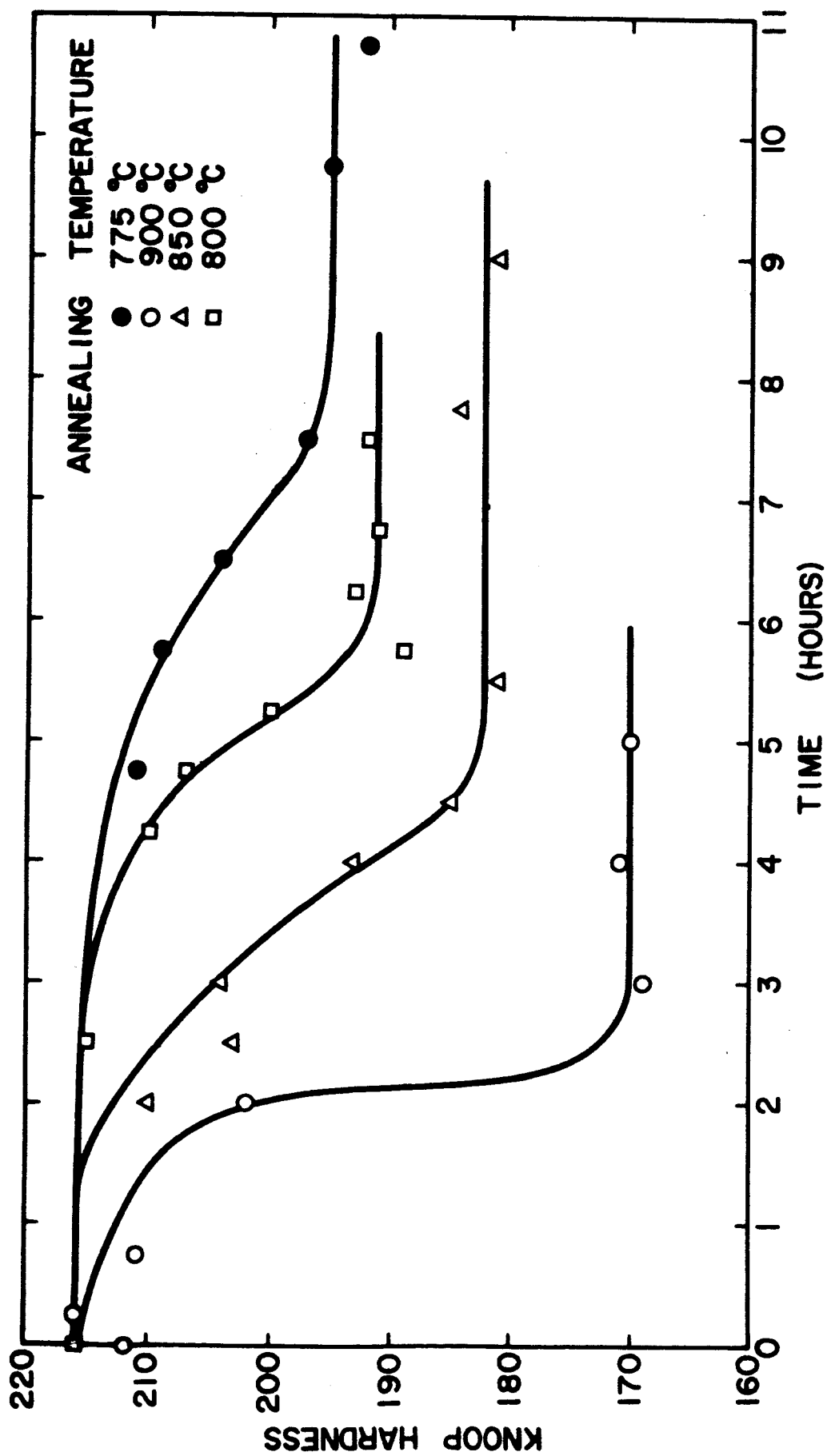


FIGURE 6. ANNEALING CURVES FOR
Ag-20% Mg ALLOY OXIDIZED AT 700°C

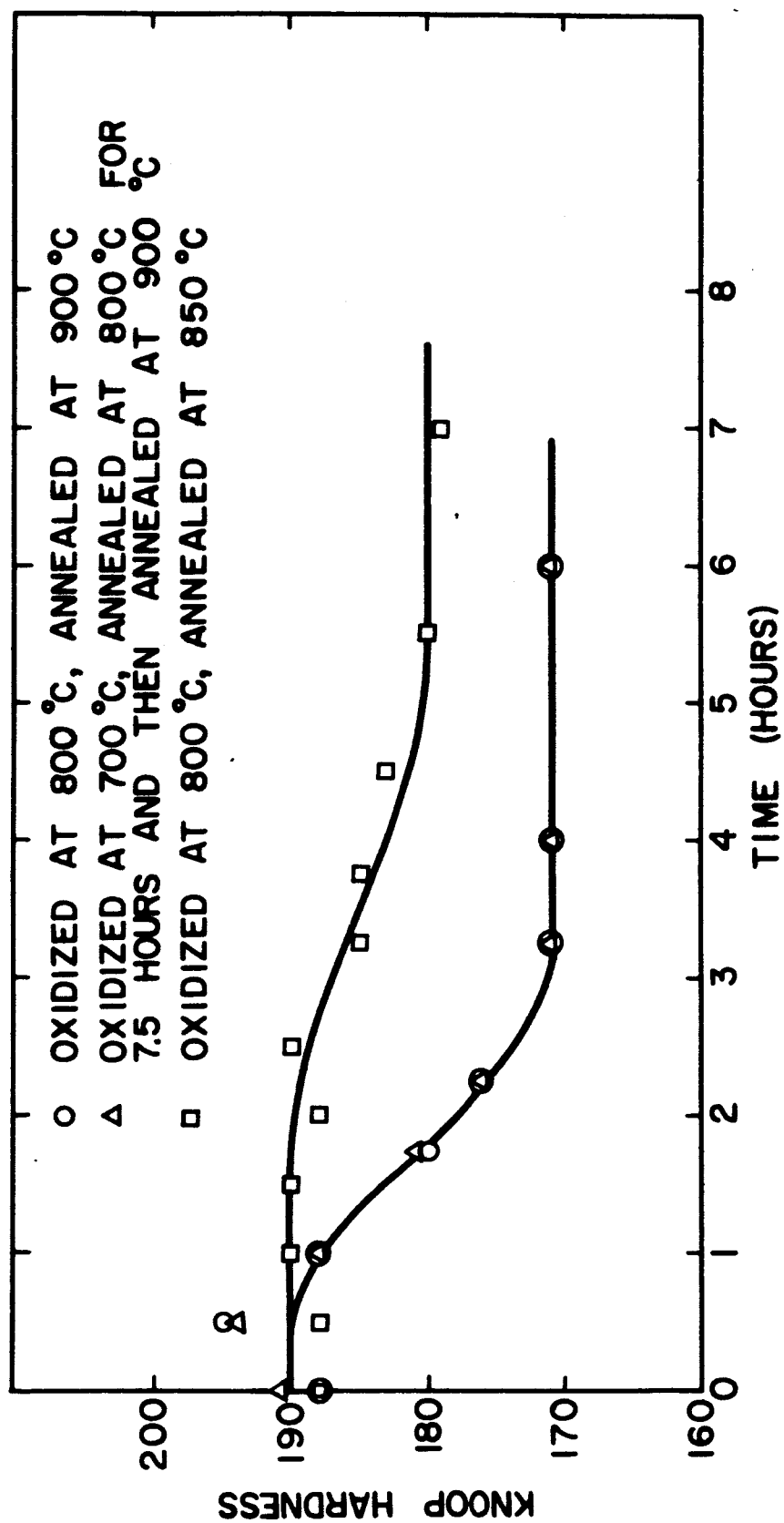


FIGURE 7. ANNEALING CURVES FOR Ag-2.0 % Mg ALLOY OXIDIZED OR PRE-ANNEALED AT 800 °C

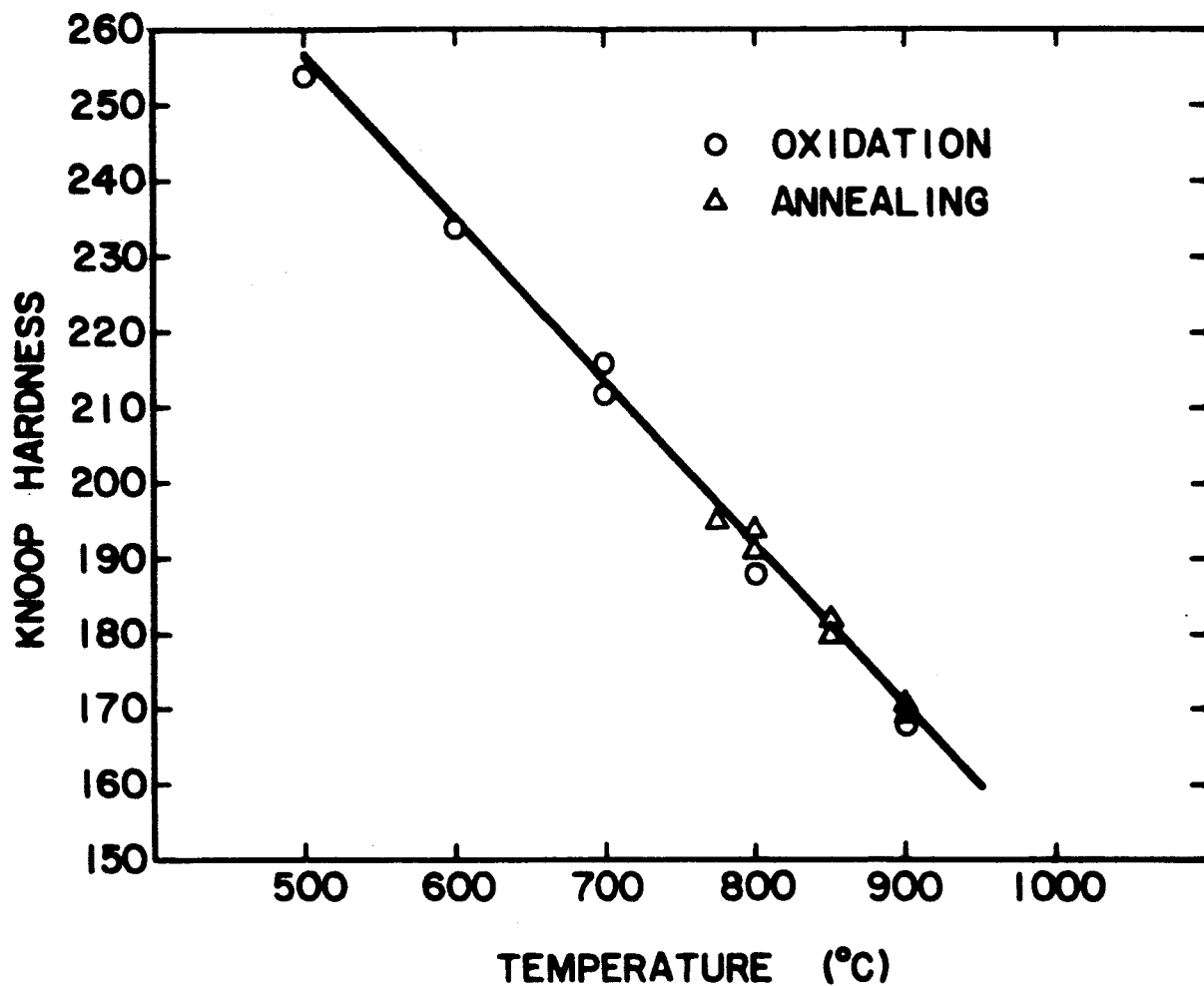


FIGURE 8. HARDNESS VERSUS OXIDATION AND ANNEALING TEMPERATURE FOR Ag-20% Mg ALLOY

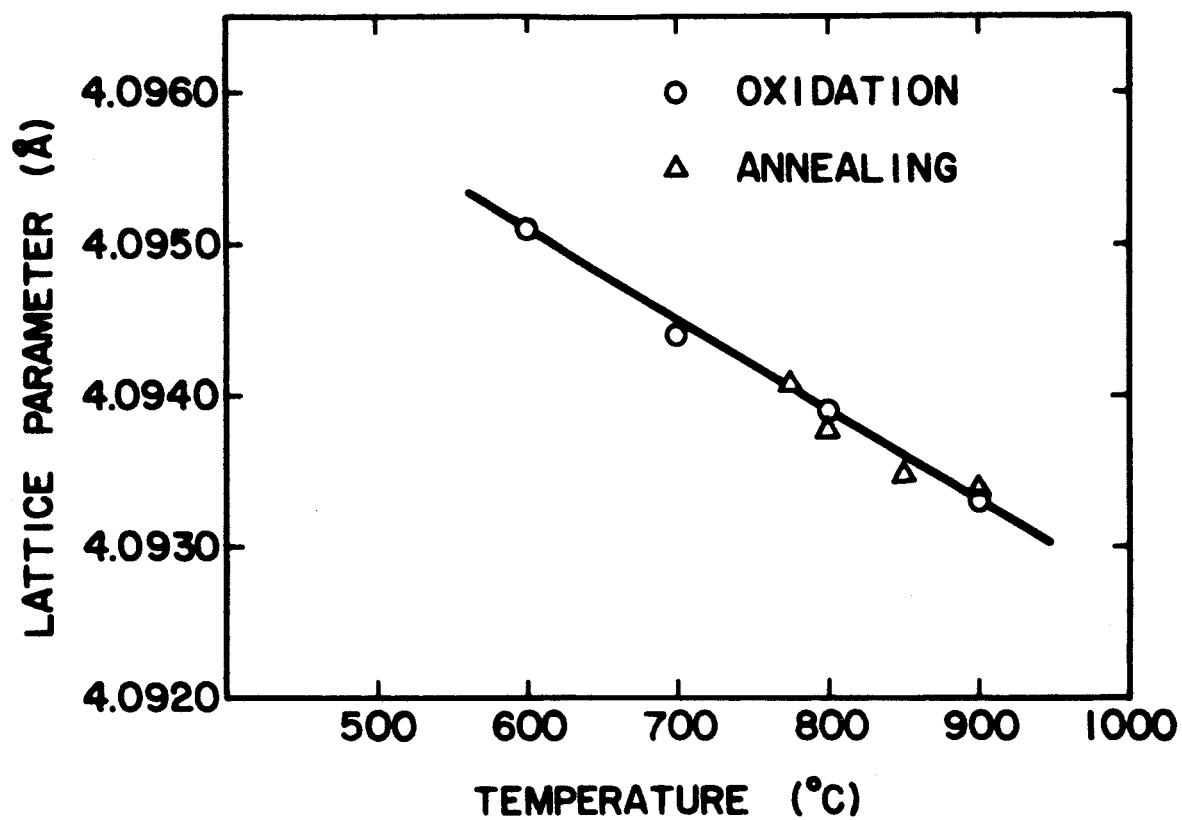


FIGURE 9. LATTICE PARAMETER VERSUS OXIDATION AND ANNEALING TEMPERATURE FOR Ag-2.0 % Mg ALLOY



Figure 10. Electron micrograph of Ag-2 ^{a/o} Mg alloy internally oxidized at 900°C. (111,000X)

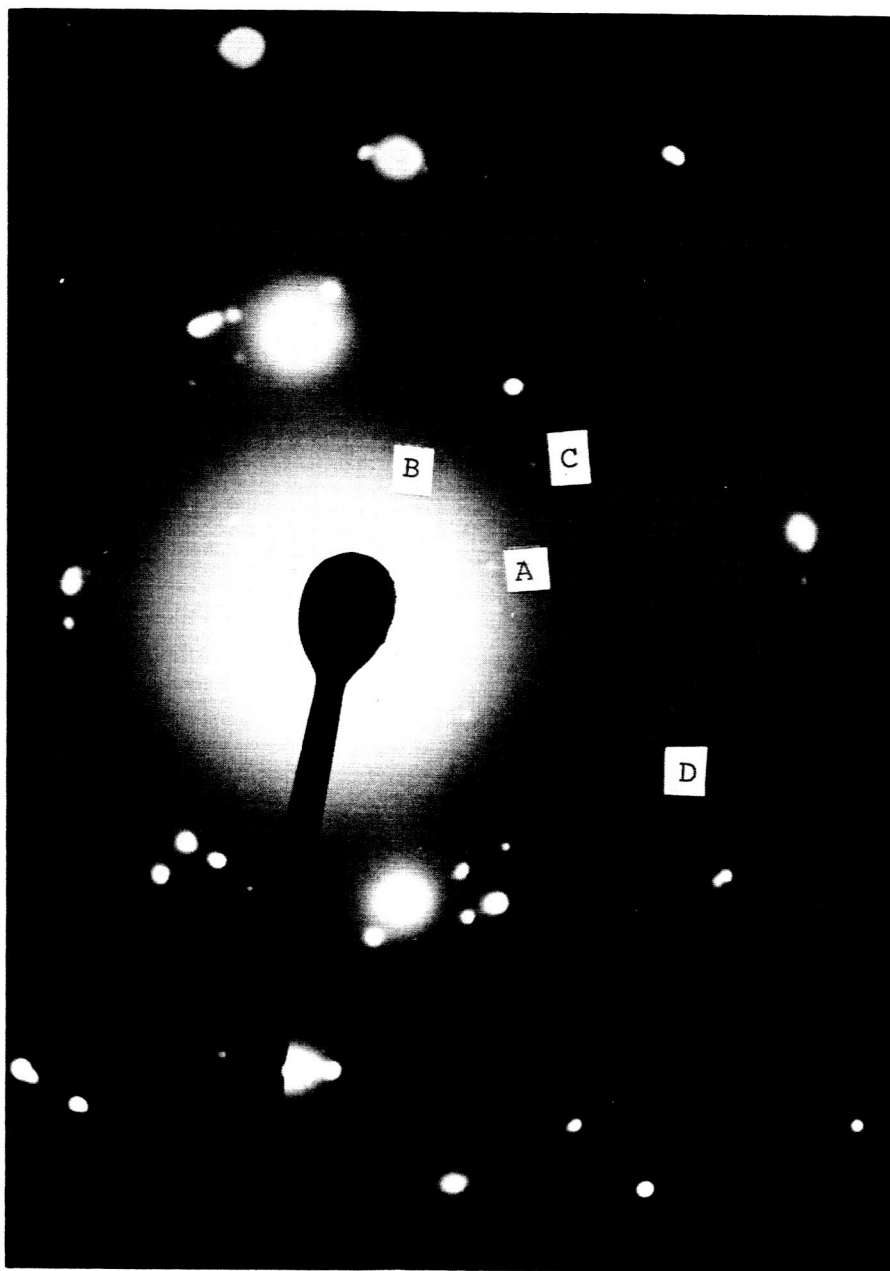


Figure 11. Electron diffraction pattern of Ag-2 at% Mg alloy internally oxidized at 900°C; points A, B, and C correspond to (220), (311), and (222) type reflections from oxide phase and point D denotes ring passing through (200) diffraction spots from matrix. (2.4 X)

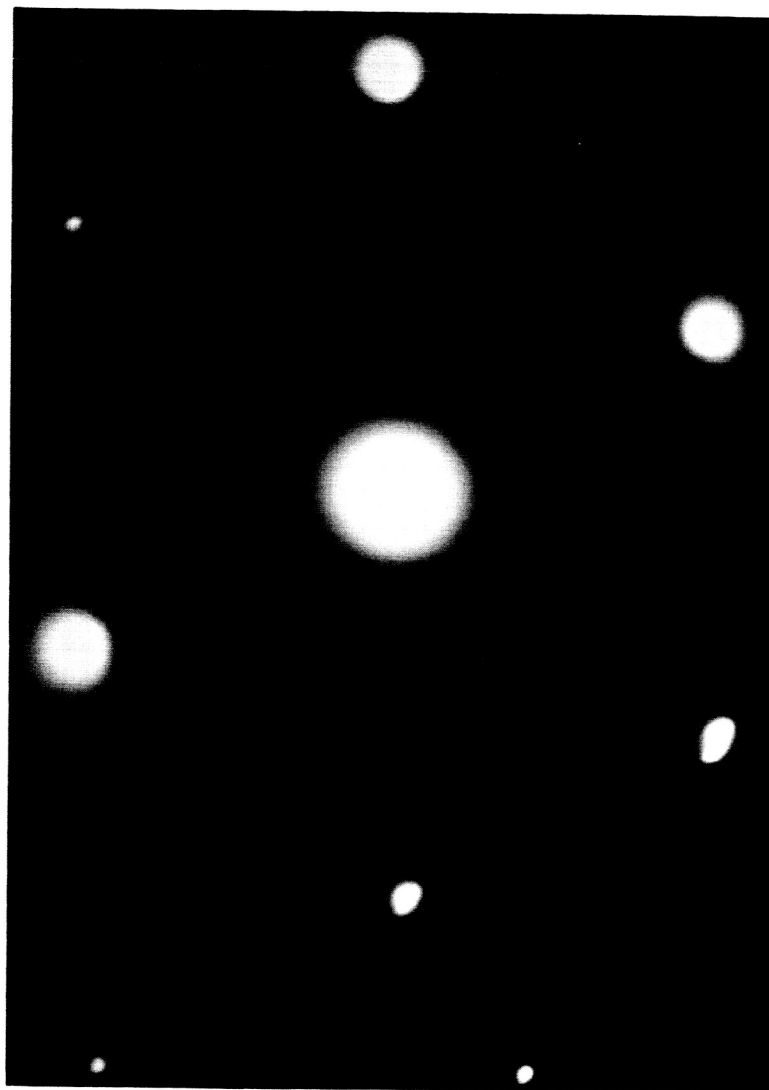


Figure 12. Electron diffraction pattern of annealed unoxidized Ag-2 ^a/o Mg alloy. (2.2X)

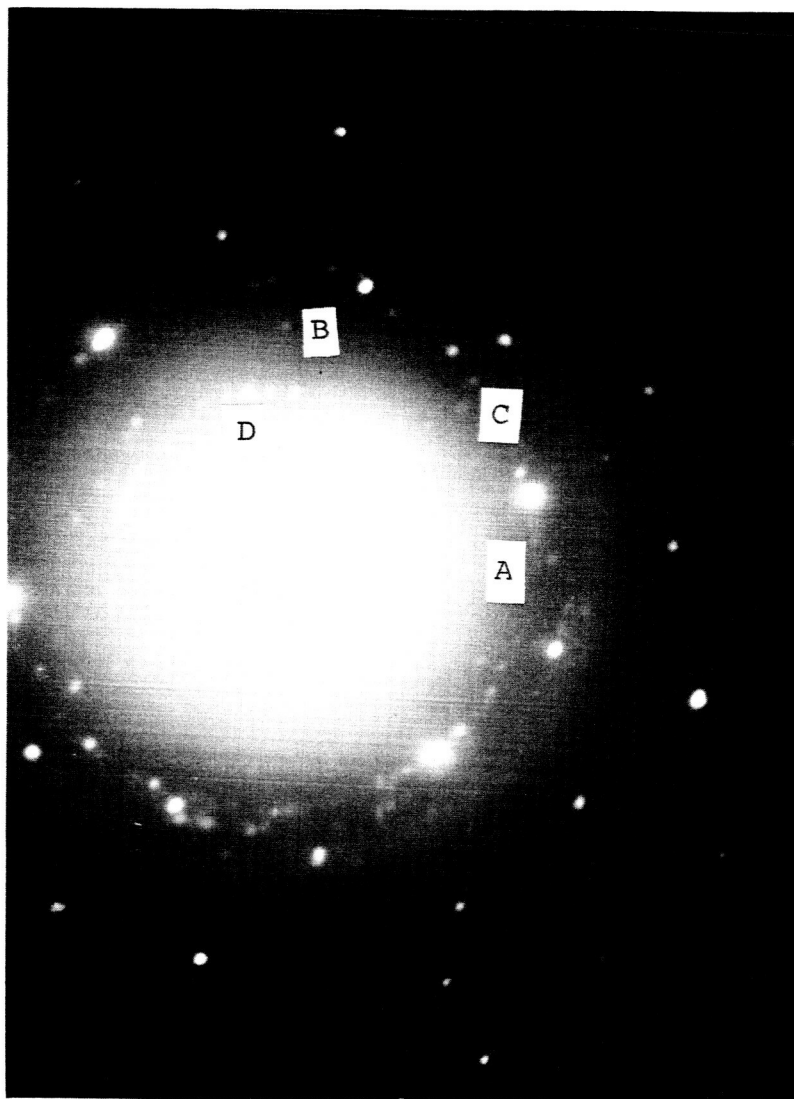


Figure 13. Electron diffraction pattern of Ag-2 ^a/o Mg alloy internally oxidized at 600°C and annealed at 900°C for 6 1/4 hours; points A, B, and C correspond to (400), (331), and (420) type reflections from oxide phase and point D denotes (111) ring from matrix.
(3 X)